Portability of Oxidase Domains in Nonribosomal Peptide Synthetase Modules†

Tanya L. Schneider and Christopher T. Walsh*

Department of Biological Chemistry and Molecular Pharmacology, Harvard Medical School, Boston, Massachusetts 02115

Received September 1, 2004; Revised Manuscript Received October 6, 2004

ABSTRACT: Oxazole and thiazole rings are present in numerous nonribosomal peptide natural products. Oxidase domains are responsible for catalyzing the oxidation of thiazolines and oxazolines to yield fully aromatic heterocycles. Unlike most domains, the placement of oxidase domains within assembly line modules varies. Noting this tolerance, we investigated the portability of an oxidase domain to a heterologous assembly line. The epimerase domain of PchE, involved in pyochelin biosynthesis, was replaced with the oxidase domain from MtaD, involved in myxothiazol biosynthesis. The chimeric module was expressed in soluble form as a flavin mononucleotide-containing flavoprotein. The functionality of the inserted oxidase domain was assayed within PchE and in transfer of the growing siderophore acyl chain from PchE to the next downstream module. While pyochelin-like product release was not observed downstream, the robust activity of the transplanted oxidase domain and the ability of the chimeric module to produce an advanced intermediate bound to the synthetase underscore the possibility of future engineering within nonribosomal peptide synthetase pathways using oxidase domains.

The five-membered ring imidazole heterocycle is a key functional group in the proteinogenic amino acid histidine. In contrast, the cognate oxazole and thiazole five-membered ring heterocycles are not typically found in proteins biosynthesized on ribosomal machinery. The *Escherichia coli* Microcin B17 peptide represents a rare exception; the 43-residue peptide is derived by proteolysis of a proprotein precursor after post-translational modification reactions that convert four cysteine and four serine residues to thiazoles and oxazoles, respectively (*1*).

Oxazole and thiazole rings, at dihydro, tetrahydro, and fully aromatized oxidation states, are found in nonribosomal peptide (NRP) natural products such as the iron-chelating siderophores pyochelin from *Pseudomonas aeruginosa* and vibriobactin from *Vibrio cholerae* (Figure 1) (*2*−*4*). Heterocyclization occurs during peptide chain elongation by multimodular nonribosomal peptide synthetases (NRPSs)[1] (*5*, *6*), catalyzed by cyclization (Cy) domains that carry out peptide bond formation, cyclization, and dehydration steps to convert *N*-acyl serine residues to oxazolines, *N*-acyl threonine to methyloxazolines, and *N*-acyl cysteine residues to thiazolines (Figure 2A) (*7*). Processing of two cysteine residues by two tandem Cy-A-T modules in an NRPS assembly line will yield a bithiazolinyl tandem linkage.

Natural products of polyketide (PK) and NRP mixed lineage are constructed by hybrid assembly lines containing mixtures of polyketide synthase (PKS) and NRPS modules (*8*). These include the 16-membered ring methylthiazolylmethylacrylyl macrolactones of the antitumor epothilone series (*9*, *10*) and the bithiazole-containing myxothiazol (*11*), both from myxobacteria. The bithiazole moiety of the hybrid antitumor drug bleomycin is a targeting element that can either intercalate or bind to the minor groove of DNA to enable single- and double-strand cleavage (*12*−*14*). The most spectacular of the peptide heterocyclic arrays may be the nanomolar inhibitor of telomerase action, telomestatin, with eight heterocycles incorporated in a macrocyclic lactam ring (*15*, *16*).

Control of the redox state of the heterocycles derived by enzymatic closure of the *N*-acyl-Ser, *N*-acyl-Thr, and *N*-acyl-Cys moieties is adjusted by tailoring enzymes or tailoring domains that affiliate with the assembly line enzymatic machinery. Reduction of the initial dihydro heterocycles, such as the thiazolines in pyochelin or yersinibactin, a hybrid PK−NRP siderophore from the plague bacterium *Yersinia pestis*, to the tetrahydro thiazolidines is effected by dedicated reductase catalytic domains, PchG and YbtU, respectively, acting *in trans* during chain elongation steps (*17*, *18*). Oxidation of the initial thiazolines or oxazolines also is observed; in these cases, oxidation is catalyzed by flavin-containing oxidase (Ox) domains embedded *in cis* as in the EpoB subunit of the epothilone synthase assembly line (Figure 3A) (*19*).

Inspection of the PKS−NRPS hybrid assembly lines for myxothiazol and bleomycin compared to the EpoB subunit, as shown in Figure 3A, raises questions about the possible portability of the Ox domain. The placement of the Ox domain within a module seems to have two options. One locale is to embed within the 50-kDa adenylation (A) domain, between the A_8 and A_9 signature motif sequences (*20*), as in EpoB and MtaD. The other is the terminal domain of a module, as in MtaC and BlmIII (*11*, *12*). This flexibility of

† T.L.S. is supported by Postdoctoral Fellowship Grant PF-02-023-01-CDD from the American Cancer Society. This work was supported by NIH Grants 20011 and AI042738 to C.T.W.

* To whom correspondence should be addressed. Phone: 617-432-1715. Fax: 617-432-0438. E-mail: christopher_walsh@hms.harvard.edu.

[1] Abbreviations: NRPS, nonribosomal peptide synthetase; PKS, polyketide synthase; Cy, cyclization; Ox, oxidase; A, adenylation; FMN, flavin mononucleotide; HPLC, high-pressure liquid chromatography; MALDI−TOF MS, matrix-assisted laser desorption ionization−time-of-flight mass spectrometry; T, thiolation; TE, thioesterase; NADPH, nicotinamide adenine dinucleotide phosphate hydride; NAC, *N*-acetylcysteamine.

10.1021/bi0481139 CCC: $27.50
Published on Web 11/25/2004

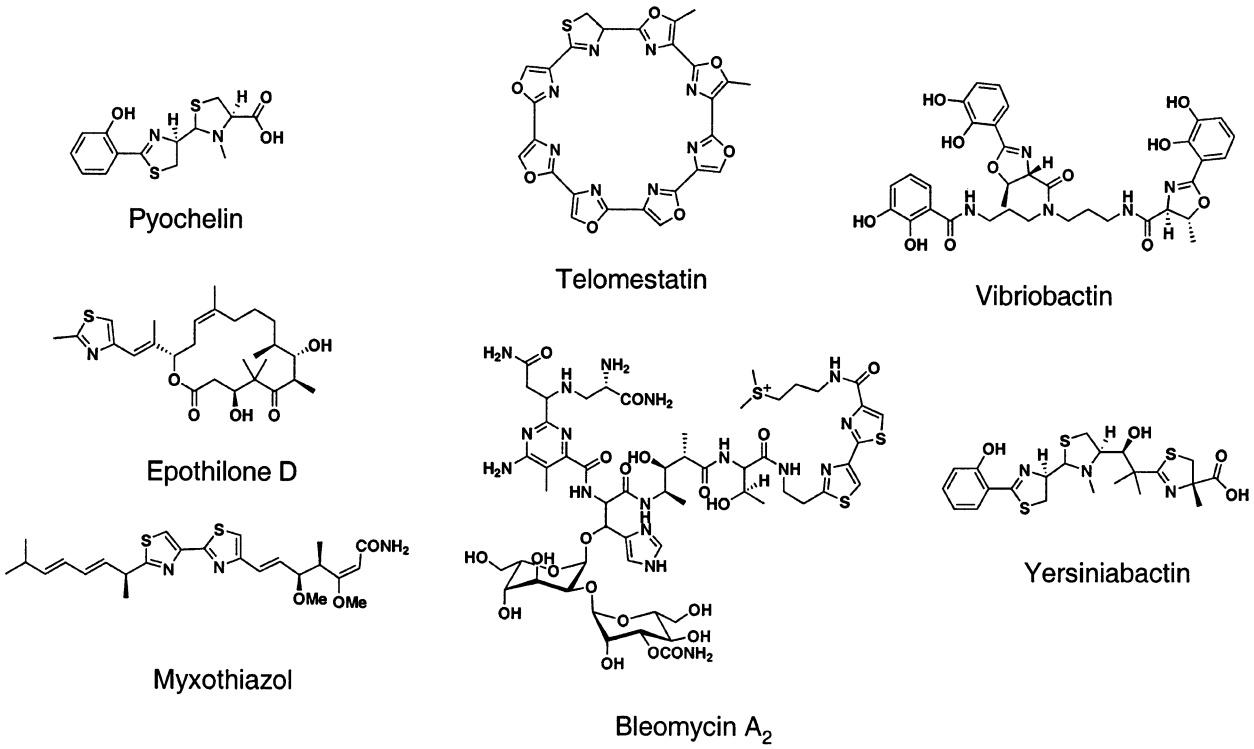

FIGURE 1: Examples of heterocycle-containing natural products.

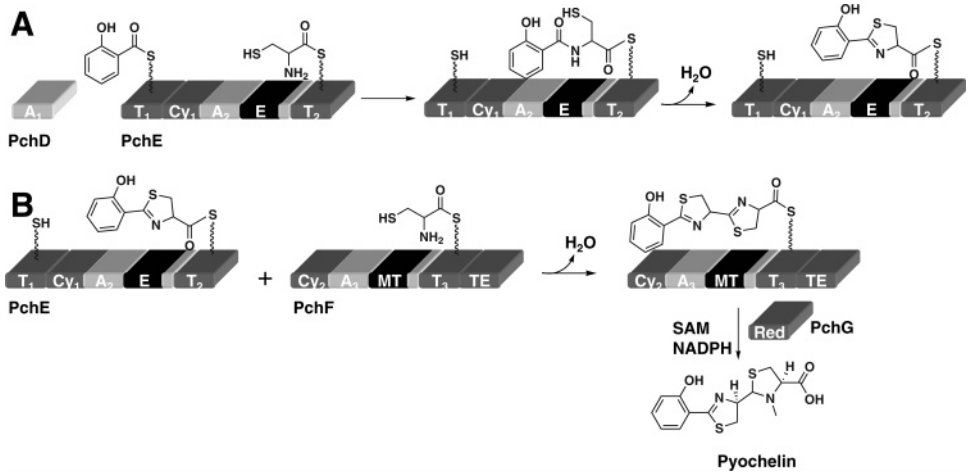

FIGURE 2: (A) Illustration of bond formation, cyclization, and dehydration as catalyzed by Cy domains. Shown are early steps in pyochelin biosynthesis on the PchE module. (B) Later steps in pyochelin biosynthesis as catalyzed by PchF and PchG.

domain location suggests that portability of Ox domains should be evaluated experimentally.

In this work, we subcloned and expressed the Ox domain from the MtaD subunit in *E. coli* and assayed it with thiazolinyl-*S*-NAC model substrates. We used this active domain to investigate the portability of an Ox domain to a heterologous assembly line, inserting the MtaD Ox domain between the A_8 and A_9 motifs of the A domain of the PchE subunit of pyochelin synthetase (*2*). PchE in its native context has an epimerase domain inserted into this A domain (*21*); thus, essentially, we conducted a domain replacement. The resulting chimeric module was expressed and purified as a flavin mononucleotide (FMN)-containing protein. The functionality of the transplanted Ox domain was assayed within PchE and in transfer of the growing siderophore acyl chain from PchE to the next downstream module PchF (*2*). The robust activity of the transplanted Ox domain and the ability of the chimeric module to function as a synthetase underscore the possibility of future engineering within NRPS pathways using Ox domains.

MATERIALS AND METHODS

General Procedures. Chemically competent *E. coli* TOP10 and BL21(DE3) cell strains were purchased from Invitrogen. Restriction endonucleases and T4 DNA ligase were purchased from New England Biolabs. The DNA polymerase Pfu Turbo (Stratagene) was used for all PCR amplification. The pET24b overexpression vector was purchased from Novagen. Oligonucleotides for PCR amplification were prepared by Integrated DNA Technologies. Reverse-phase high-pressure liquid chromatography (HPLC) analysis of enzyme reaction products was performed on a Beckman System Gold with a Vydac C18 column (100 Å, 4.6 × 250 mm). The Beckman system was connected in tandem with a Beckman 171 Radioisotope Detector for radioHPLC analysis. MALDI−TOF MS (matrix-assisted laser desorption

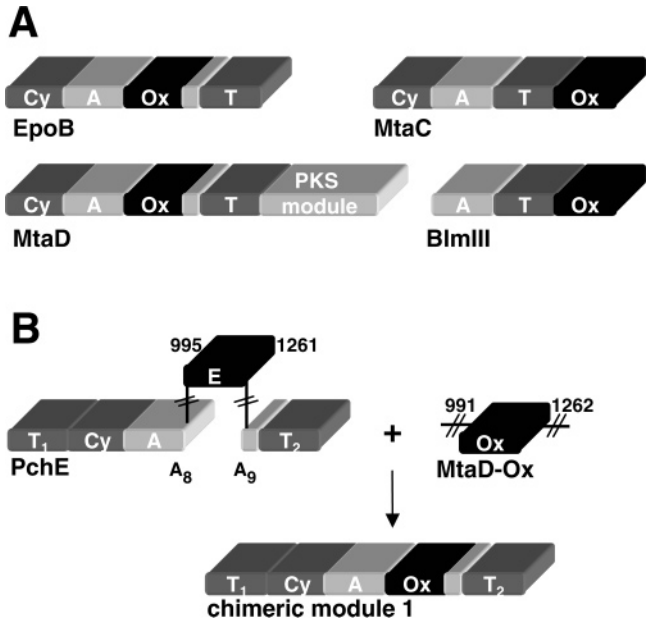

FIGURE 3: (A) Varied placement of Ox domains within NRPS modules. These NRPS modules are involved in epothilone biosynthesis (EpoB), myxothiazol biosynthesis (MtaC and MtaD), and bleomycin biosynthesis (BlmIII). (B) Design of chimeric module **1** by insertion of the MtaD-Ox domain in place of the E domain within PchE.

ionization−time-of-flight mass spectrometry) was performed at a Voyager-DE STR BioSpectrometry Workstation (PerSeptive Biosystems). UV−vis spectra were collected on a Hewlett−Packard 8453 spectrophotometer.

*Cloning of MtaD-Ox Domain and Chimeric Module **1***. The mtaD-Ox fragment (nucleotides 2971−3786 of *mtaD*) was amplified by PCR from a plasmid prepared in the pCYB2 vector containing a portion of the *mtaD* sequence. This plasmid was a gift from Rolf Müller's laboratory (Saarland University, Saarbruecken, Germany). The forward primer was designed to incorporate an *Nde*I site, and the reverse primer incorporated a *Not*I site into the amplified sequence. Amplified products were digested and ligated into a linearized pET24b vector to give pMtaD-Ox. DNA sequencing confirmed the correct insertion of the gene into the vector.

The plasmid coding for the production of chimeric module **1** was prepared using the technique of splicing by overlap extension (SOE) (*22*). Because chimeric module **1** is comprised of N- and C-terminal portions of PchE with inserted MtaD-Ox between, three sets of primers were designed to amplify each of these segments. The primers were also designed to include overlaps and restriction sites where appropriate. Nucleotides 2586−2983 of pchE were amplified using primers pchE1 (5′-GATTCCCTACGGCCGGCCATTGCCGGGA-3′) and pchEM2 (5′-GTGCTCGCCGAGGGCGCGCTTGGCGCCAGGCGCGGTACCAG-3′). pchE1 included the *Fse*I site needed for cloning this fragment back into the pPchE vector after mtaD-Ox insertion, and pchEM2 included an overlapping sequence with the mtaD-Ox sequence. The mtaD-Ox sequence to be inserted (nucleotides 2971−3786) was amplified using primers mtaDOx1 (5′-CTGGTACCGCGCCTGGCGCCAAGCGCGCCCTCGGCGAGCAC-3′) and mtaDOx2 (5′-CGCCAATCCCGCAGCGGCGAGGAATTCCAGTGAAGCATCCGC-3′), both including an overlap with the pchE sequence. A final portion of pchE, nucleotides 3784−4349, was amplified using primers pchEM3 (5′-GCGGATGCTTCACTGGAATTCCTCGCCGCTGCGGGATTGGCG-3′) and pchE4XhoI (5′-GGTGGTGGTGCTCGAGTGCGGCCGCAAGC-3′), providing the *Xho*I site for cloning back into linearized pPchE. After all three segments were amplified using the primers described above, the PCR products were agarose-gel-purified and collectively used as the template in a subsequent PCR reaction with pchE1 and pchE4XhoI as primers. The spliced, complete insert was agarose-gel-purified and digested with *Fse*I and *Xho*I. The insert was ligated into pPchE (*2*) that had been digested with *Fse*I and *Xho*I, thus removing the original nucleotides 2602−4335 and replacing them with the insert containing the oxidase domain. DNA sequencing confirmed that the desired construct, pchimera1, was prepared.

*Overexpression and Purification of MtaD-Ox and Chimeric Module **1***. BL21(DE3) cells were transformed with pMtaD-Ox plasmid and grown in LB media (3 × 1 L) supplemented with 30 μg/mL kanamycin. Cultures were grown to OD_{600} = 0.8 at 37 °C; protein expression was induced by the addition of isopropyl-β-D-thiogalactopyranoside (IPTG) to 100 μM; growth continued for an additional 3.75 h at 25 °C. Harvested cells were resuspended in 25 mL of lysis buffer (25 mM Tris at pH 8.0, 200 mM NaCl, and 10% (v/v) glycerol) and lysed by French Press. Cell lysate was clarified by centrifugation, and the resulting supernatant was incubated with 1 mL of Ni−NTA resin (Qiagen) for 3 h at 4 °C. The resin was decanted into a column and washed with 20 mL of 5 mM imidazole in lysis buffer. C-terminally His_6-tagged MtaD-Ox protein was eluted with a step gradient of 30, 60, 100, 250, and 500 mM imidazole in lysis buffer. Fractions containing MtaD-Ox as judged by SDS−PAGE were pooled and dialyzed against lysis buffer (2 × 2 L). Purified MtaD-Ox was bright yellow, and the enzyme concentration was calculated based on the known extinction coefficient for FMN, 12 200 cm^{-1} M^{-1} at 450 nm (*23*). MtaD-Ox samples were heat-denatured for 2 min at 90 °C, and the supernatant was subjected to UV−vis analysis. The total yield of pure protein, calculated based on flavin content, was typically 2 mg/L. Fractional loading of protein with FMN was determined by calculating the difference in absorbance at 280 nm for the native protein and for released FMN following heat denaturation of the protein to give the protein concentration based on absorbance at 280 nm. This protein concentration was then compared with the total flavin content, based on A_{450} analysis of the released flavin, to give fractional protein loading.

For the overproduction of N-terminally His_6-tagged chimeric module **1**, BL21(DE3) cells were transformed with pchimera1 plasmid. Cultures were grown in LB media (3 × 1 L) supplemented with 30 μg/mL kanamycin to OD_{600} = 0.4 at 37 °C. Cultures were cooled to 15 °C, while growth continued for an additional hour. Protein expression then was induced with the addition of IPTG to 60 μM, and expression continued for 18 h at 15 °C. Harvested cells were resuspended in 35 mL of lysis buffer and lysed using a cell disrupter (Emulsiflex-C5, Avestin). Cell lysate was clarified by centrifugation, and the resulting supernatant was incubated with 3 mL of Ni−NTA resin for 2 h at 4 °C. The resin was decanted into a column and washed with 25 mL of lysis buffer. Chimeric module **1** was eluted with a step gradient from 5 to 500 mM imidazole in lysis buffer. Again, fractions

containing desired protein as judged by SDS−PAGE were pooled and dialyzed against lysis buffer. Traces of a copurifying contaminant protein were detected, as previously reported with PchE overexpression (*17*). Purified **1** was yellow, and the enzyme concentration was calculated based on FMN content in this case as well. The total yield of protein was typically 6 mg/L.

Overexpression and purification of PchD, PchF, PchFTE, and PchG for use in reconstitution assays were performed as previously described (*2*, *24*).

*Covalent Incorporation of Phosphopantetheine into PchE, **1**, and PchFTE*. Proteins were converted from the apo to holo form following previously determined procedures (*25*). Each protein (between 2 and 15 μM) in buffer (50 mM Tris at pH 7.5, 5 mM $MgCl_2$, and 5 mM TCEP) was primed with CoA (150 μM) as catalyzed by the phosphopantetheinyl transferase Sfp (5 μM). Reactions proceeded at 25 °C for 1 h.

*ATP-[^{32}P]Pyrophosphate Exchange Reactions by **1***. ATP−PP_i exchange catalyzed by **1** was measured as described previously (*2*) to allow direct comparison with values measured for PchE. In brief, 100 μL of reaction mixtures contained 75 mM Tris at pH 8.8, 10 mM NaCl, 1 mM sodium [^{32}P]pyrophosphate, 2 mM dithiothreitol, and 5% glycerol. The concentration of cysteine was varied for the determination of kinetic parameters. Chimera **1** was added to the reaction at a final concentration of 1.2 μM, and reactions were initiated with the addition of ATP to 5 mM. After incubation for 30 min at 30 °C, reactions were quenched by the addition of 0.5 mL of a charcoal suspension [1.6% (w/v) activated charcoal, 0.1 M tetrasodium pyrophosphate, and 0.35 M perchloric acid]. The charcoal was pelleted by centrifugation, washed 3 times with 1 mL of 0.1 M tetrasodium pyrophosphate and 0.35 M perchloric acid, resuspended in 0.5 mL of water, and subjected to liquid scintillation counting (LS6500, Beckman Coulter).

*Covalent Incorporation of [^{14}C]Cysteine into **1** or PchE*. Cysteinylation of **1** or PchE with time was measured in reaction mixtures containing 75 mM Tris at pH 7.5, 10 mM $MgCl_2$, 1.5 mM [^{14}C]cysteine (1.8 μCi/μmol), and 4.3 μM holo **1** or 2.15 μM holo PchE. Reactions were initiated with the addition of 1 mM ATP, and aliquots (50 μL) of the reaction mixture were removed with time and quenched with 0.75 mL of 10% TCA. Protein pellets were washed twice with 10% TCA, resuspended in 100 μL of formic acid, and subjected to liquid scintillation counting for analysis.

Oxidase Activity Assays. Reactions containing MtaD-Ox or **1** were carried out in 75 mM sodium phosphate at pH 7 and 25 °C. Phenylthiazolinyl-*S*-NAC substrate was prepared as previously described (*19*). Reactions were initiated by the addition of oxidase (1.5 μM **1** or 0.38 μM MtaD-Ox) and quenched by heat denaturation at 90 °C for 2 min. Reaction products were detected by analytical HPLC and quantified as described (*19*).

*Production and Detection of Pyochelin-like Intermediates: PchD with **1** or PchE*. Reactions to probe the products formed upon combination of PchD (9.7 μM) with PchE (2 μM), PchE and MtaD-Ox (each 2 μM) or **1** (2 μM) were executed in buffer containing 75 mM Tris at pH 7.5, 10 mM $MgCl_2$, 1 mM benzoate, and 20 μM [^{14}C]cysteine (300 mCi/mmol). Both benzoate and salicylate are acceptable substrates for PchE (*21*). Reactions (200 μL) were initated by the addition of 1 mM ATP and quenched after 2 h at 25 °C with the addition of 0.75 mL of 10% TCA. Protein pellets were washed twice with 10% TCA, then dissolved in 100 μL of 0.1 M KOH, and heated at 60 °C for 10 min. Trifluoroacetic acid (50%, 5 μL) was added, and the solutions were centrifuged to remove precipitated proteins. Chemically synthesized standards were added to the radioactive enzymatic reactions, and the mixtures were analyzed by radio-HPLC. Dual on-line UV (254 nm) and radioisotope (tuned for ^{14}C) detectors were used to monitor the retention time of standards and radioactive enzymatic products, respectively. Separation was effected using a gradient of 0−100% buffer B (acetonitrile) in buffer A (0.1% TFA in water) over 25 min at 1 mL/min.

Production and Detection of Intermediates with PchFTE Added: Chain Elongation. Further assays were performed to investigate the products resulting when PchFTE (0.6 μM) was added to the reaction mixtures described above. Here, reactions proceeded for 2.5 h before quenching and hydrolysis as described above. HPLC separation was effected using a gradient of 10−60% buffer B (acetonitrile) in buffer A (0.1% TFA in water) over 25 min at 1 mL/min.

Reconstitution of Pyochelin Biosynthesis. PchD (2 μM), apo PchE (2.5 μM) or **1** (5 μM), apo PchF (2.5 μM), and PchG (6 μM) were combined in buffer [37.5 mM Tris at pH 7.5, 10 mM $MgCl_2$, 0.1 mM CoA, 1 mM salicylate, 5 mM cysteine, 2 mM *S*-adenosylmethionine, and 2 mM nicotinamide adenine dinucleotide phosphate hydride (NADPH)] with Sfp (2.7 μM) to catalyze protein priming. After 1 h, 3 mM ATP was added to initiate the reconstitution reaction. Samples (100 μL) were quenched after 18 h with the addition of 10 μL of 1 N HCl. Salicylate-containing compounds were extracted with 800 μL of ethyl acetate. The organic fraction was dried, resuspended in 300 μL of 30% acetonitrile, and analyzed by HPLC. HPLC separation was effected using a gradient of 10−100% buffer B (acetonitrile with buffer A in a 4:1 ratio) in buffer A (0.1 mL of formic acid and 0.2 mL of TEA in 1 L of water) over 23 min at 1 mL/min.

Preparation of Chemically Synthesized Standards. 2-Phenylthiazoline-4-carboxylic acid and 2-phenylthiazole-4-carboxylic acid were prepared and characterized as described (*19*). 2-Phenylthiazolinyl-cysteine was prepared and characterized as described (*26*). 2-Phenylthiazolyl-cysteine was prepared by coupling 2-phenylthiazole-4-carboxylic acid (1 equiv) with cysteine methyl ester (1.5 equiv) in the presence of PyBOP [(benzotriazol-1-yloxy)tripyrrolidinophosphonium hexafluorophosphate, 1.5 equiv] and triethylamine (3 equiv) in dichloromethane. The reaction was complete after 2 h, and the desired product was purified using preparative reverse-phase HPLC. Cleavage of the methyl ester was executed as described for phenylthiazolinyl-cysteine (*26*). Identity of cleavage products was confirmed by MALDI−TOF MS (For phenylthiazolinyl-cysteine, $[M+H]^+$: observed, 311.1; calculated, 311.4. For phenylthiazolyl-cysteine, $[M+H]^+$: observed, 309.2; calculated, 309.4).

RESULTS

Design, Expression, and Purification of PchE/MtaD-Ox Chimeric Module. The heterologous expression of the five-domain PchE protein from the pyochelin biosynthesis gene cluster has been described (*2*). As seen in Figure 3B, PchE

contains an epimerase (E) domain inserted between the conserved A_8 and A_9 motifs of the A domain (*5*). Here, we describe the design and analysis of a chimeric module based on PchE. In this novel construct, the E domain was removed and replaced with the Ox domain from MtaD, a hybrid NRPS/PKS protein involved in the biosythesis of myxothiazol (*11*). In designing the resulting chimeric module **1**, care was taken that the inserted MtaD-Ox domain did not destroy the integrity of the PchE protein and that insertion in a foreign module did not render the MtaD-Ox domain inactive. To this end, the insert sites within the PchE module (residues 995−1261) were chosen based on secondary structure predictions describing the unstructured flanking regions around the E domain. The MtaD-Ox domain was identified based on sequence alignment with other Ox domains, and the soluble MtaD-Ox domain (residues 991−1262 of MtaD) was expressed with a C-terminal His_6 tag in *E. coli* in reasonable yield (2 mg/L). Because this isolated domain was shown to be active with the FMN cofactor bound, it was chosen for insertion into PchE. Thus, PchE residues 995−1261 were replaced by residues 991−1262 of MtaD to yield module **1** (Figure 3B).

Module **1** was expressed with an N-terminal His_6 tag in *E. coli* in good yield (6 mg/L). It was necessary to express **1** at 15 °C to obtain soluble protein, which was purified using nickel-affinity chromatography (Figure 4A). Purified **1** was yellow, indicating that the FMN cofactor was bound by the protein. The presence of FMN was confirmed by UV−vis spectroscopy (Figure 4B) and HPLC analysis after heat denaturation of **1**. The protein was approximately 72% loaded with FMN, as compared to 100% for isolated MtaD-Ox.

Characterization of Individual Domains Within Module 1. Individual domains of **1** were analyzed to assess the impact of the domain swap on their activity. The A domain, the site of the swap, was investigated first by measuring the activation of cysteine monomers as adenylates. The cysteine-dependent exchange of radiolabeled inorganic pyrophosphate ($[^{32}P]PP_i$) into ATP was determined and compared with the kinetic parameters measured for PchE (Figure 5A) (*2*). The rate constant measured for **1** was more than an order of magnitude lower than that measured for PchE ($k_{cat} = 2.2 \pm 0.1$ min^{-1} as compared to 38 min^{-1}). Additionally, the K_m for **1** (3.0 ± 0.2 mM) was higher than that previously determined for PchE (0.11 mM), yielding an overall relative k_{cat}/K_m = 1:473 for **1** compared with PchE. While the catalytic efficiency of the A domain was compromised by the E to Ox domain swap, the A domain clearly remained active.

Cysteinylation of the **1** thiolation (T) domain was compared with that for PchE by monitoring the incorporation of $[^{14}C]$cysteine into each protein. While both T domains were loaded to saturation within a minute, in **1**, the cysteinyl-*S*-enzyme accumulated to a lesser degree (12%) than in PchE (28%; Figure 5B). The extent of fractional stoichiometry of cysteine loading for PchE was in good agreement with the previously published 27% at saturation (*2*). The reasons for substoichiometric aminoacylation in this and other A domains are not known. In conclusion, both the A and T domains derived from PchE appear to be functional albeit hampered in construct **1**.

The implanted Ox domain of **1** was also investigated. Its activity was compared with that of the excised MtaD-Ox domain using phenylthiazolinyl-*S*-NAC as a soluble substrate. Such small molecule thioester substrates had been used previously as mimics for substrates linked to the phosphopantetheinyl prosthetic group of T domains to measure Ox domain activity (*19*). Here, it was shown that the inserted Ox domain of **1** demonstrated similar activity to MtaD-Ox (Figure 5C). The activity of both Ox domains was robust, with $k_{cat} = 862.1 \pm 2.1$ and 395.9 ± 8.8 min^{-1} for MtaD-Ox and **1**, respectively. K_m values were nearly identical, equal to 1.1 ± 0.4 and 1.2 ± 0.1 mM for MtaD-Ox and **1**, respectively, yielding an overall relative k_{cat}/K_m = 2:1. While the 2-fold difference in catalytic efficiency suggests a slight impact on Ox domain integrity upon insertion into construct **1**, the Ox domain exhibited the smallest change in activity of the domains assayed within **1**.

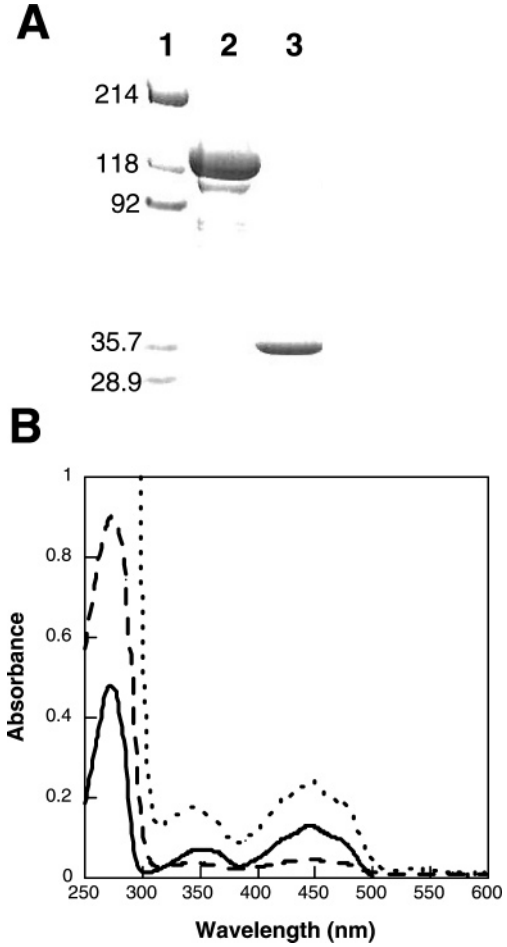

FIGURE 4: (A) SDS−PAGE analysis of protein purification by nickel-affinity chromatography. Lane 1, molecular weight markers (kDa); lane 2, purified module **1**; lane 3, purified MtaD-Ox. (B) UV−vis spectra of 11 μM purified MtaD-Ox (—), 2.5 μM purified module **1** (- - -), and 15 μM purified module **1** (···) showing the absorption maxima at 279, 349, and 445 nm that are characteristic of flavin-containing proteins.

Characterization of Synthetase Activity from Purified PchD and Module 1. The individual domains of **1** proved active, and thus the activity of the entire module in concert with the upstream A domain protein, PchD, was assessed. PchD was combined with either **1** or PchE in the presence of benzoate, ATP, and $[^{14}C]$cysteine. After 2 h, the proteins were precipitated and thioester-bound molecules were released through base hydrolysis. These small molecules were subjected to radioHPLC analysis with co-injection of chemi-

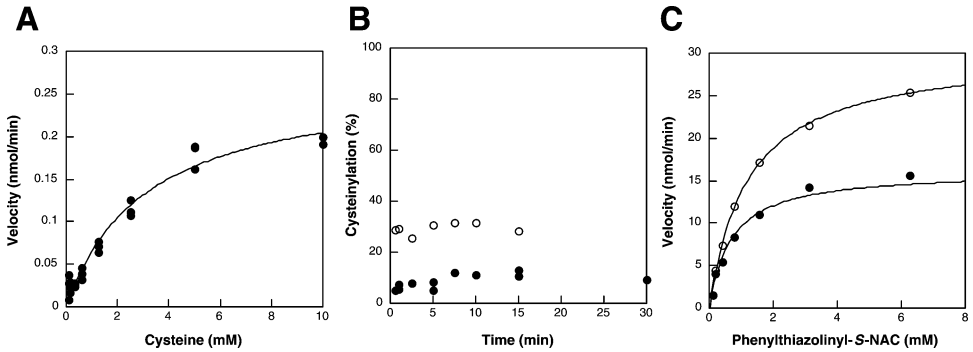

FIGURE 5: Activity of individual domains within module **1**. (A) Velocity of cysteine-dependent exchange of [^{32}P]PP$_i$ into ATP for module **1**. (B) Aminoacylation of module **1** (●) and PchE (○) with [^{14}C]cysteine. (C) Velocity of phenylthiazolinyl-*S*-NAC oxidation as catalyzed by module **1** (●) and MtaD-Ox (○).

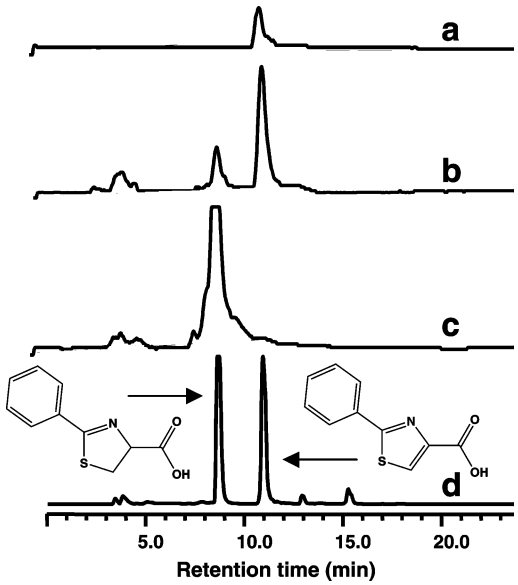

FIGURE 6: HPLC analysis and identification of enzyme incubation products released from the module **1** or PchE T domain after 2 h by KOH hydrolysis. All reactions contained benzoate, ATP, and [^{14}C]cysteine. Shown in radioHPLC traces are the products resulting from (a) the incubation of 9.7 μM PchD with 2 μM module **1**, (b) the incubation of 9.7 μM PchD with 2 μM PchE and 2 μM MtaD-Ox, and (c) the incubation of 9.7 μM PchD with 2 μM PchE. Also shown (d) are authentic standards added to the radioactive reaction mixtures and monitored by a UV detector at 254 nm.

cal standards. As shown in Figure 6, a combination of PchD with PchE produced the expected phenylthiazoline carboxylate, while a combination of PchD with **1** produced only the oxidized phenylthiazole carboxylate even at incubation times as short as 5 min (data not shown). Interestingly, the related *in trans* experiment, combining PchD with PchE in the presence of MtaD-Ox, yielded both thiazoline- and thiazole-containing products. Whether this mixture is due to inefficient *in trans* oxidation or the epimerization of the thiazoline by the PchE E domain, therefore presenting the Ox domain with the wrong substrate enantiomer (*19*), is a topic for further study. It is clear that module **1**, with the Ox domain inserted, catalyzes the accumulation of only the oxidized phenylthiazole-*S*-enzyme covalent intermediate.

*Chain Elongation: Transfer from Module **1** to PchF*. The full reconstitution of pyochelin biosythesis has been demonstrated using heterologously expressed and purified PchD, PchE, PchF, and PchG (*24*). Additionally, intermediates resulting from the combination of PchD, PchE, PchF, and appropriate substrates and cofactors have also been characterized because the thioesterase (TE) domain of PchF permits slow release of intermediates, even in the absence of reductase PchG (*2*). A construct was previously prepared (PchFTE) in which the TE domain was rendered inactive, therefore eliminating this slow release of intermediates (*2*). To test whether intermediates tethered to module **1** would be transferred to PchF, module **1** or PchE was combined with PchD and PchFTE in the presence of benzoate, ATP, and [^{14}C]cysteine. After incubation for 2.5 h, the proteins were precipitated and covalently tethered thioester-bound molecules were released through base hydrolysis. The addition of PchFTE to the reaction mixtures resulted in additional molecules detected by radioHPLC, as shown in Figure 7. With both PchE and module **1**, new product peaks coeluted with standards corresponding to cysteine addition products. It appears that the intermediate phenylthiazole tethered to the T domain of **1** is transferred to PchFTE through condensation with PchFTE-bound cysteine.

Further reconstitution was attempted by combining PchD, PchF, PchG, necessary substrates, and cofactors with module **1**. Even at long incubation times of 18 h, there was no evidence of any pyochelin-like products released by the PchF TE domain as detected by UV−HPLC at 254 nm. Conversely, the parallel control reconstitution reaction containing PchE resulted in the formation of pyochelin as shown in Figure 8 and confirmed by MALDI−TOF MS. Intermediates that accumulate on PchF with module **1** are illustrated in Figure 9. It appears likely that the change in oxidation state catalyzed by the inserted Ox domain contributed to the lack of late stage acyl-*S*-enzyme processing and hydrolytic product release.

DISCUSSION

Natural products resulting from NRPS or hybrid PKS/NRPS assembly lines often feature five-membered ring heterocycles. In addition to the imidazole ring in the proteinogenic amino acid histidine, thiazole and oxazole rings can be found in natural products produced through nonribosomal peptide synthesis. Oxidation to yield such aromatic heterocycles is catalyzed by flavin-containing Ox domains present in some NRPS modules and can impact both the integrity and bioactivity of natural products. The Ox domain catalyzes the transformation of rather labile thiazolines or oxazolines to the more stable heteroaromatic thiazoles or oxazoles. Such oxidation can also be important for the activity of natural products; the thiazoles present in both bleomycin and epothilone are needed for full potency of these

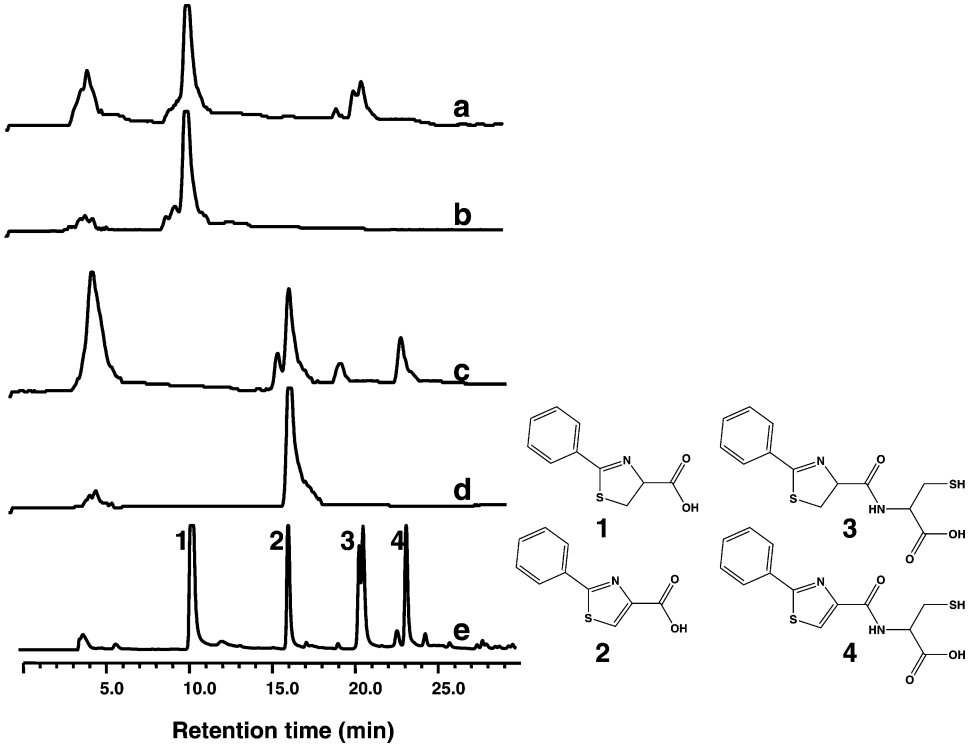

FIGURE 7: HPLC analysis and identification of enzyme incubation products released from T domains after 2.5 h by alkaline hydrolysis. All reactions contained benzoate, ATP, and [^{14}C]cysteine. Shown in radioHPLC traces are the products resulting from (a) the incubation of 9.7 μM PchD with 2 μM PchE and 0.6 μM PchFTE, (b) the incubation of 9.7 μM PchD with 2 μM PchE alone, (c) the incubation of 9.7 μM PchD with 2 μM module **1** and 0.6 μM PchFTE, and (d) the incubation of 9.7 μM PchD with 2 μM module **1** alone. Also shown (e) are authentic standards added to the radioactive reaction mixtures and monitored by a UV detector at 254 nm. The doublet seen with standard 3, phenylthiazolinyl-cysteine, likely represents two diastereomers resulting from epimerization at the thiazoline α carbon.

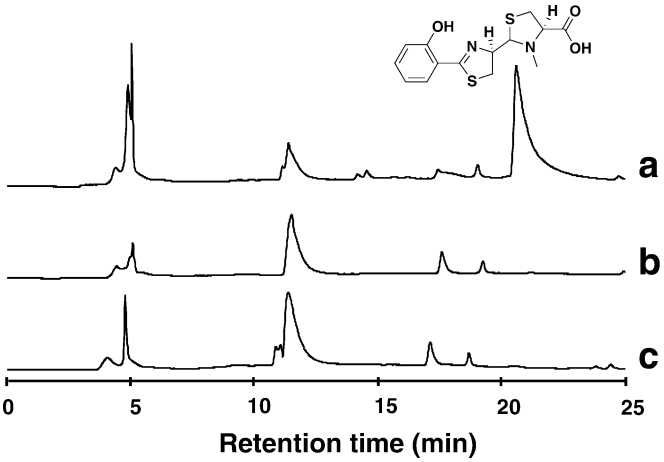

FIGURE 8: HPLC analysis and identification of pyochelin extracted from reconstitution reactions. Combination of PchD, PchE, PchF, and PchG (a) with necessary substrates and cofactors resulted in the production of pyochelin as detected at 254 nm and confirmed by MALDI−TOF MS ([M+H]$^+$: observed, 325.3; calculated, 325.4). Pyochelin was not detected in similar reactions when PchE was omitted (b) or when module **1** was substituted for PchE (c).

molecules (*14*, *27*). Because of the additional functionality that Ox domains confer upon natural products, it is interesting to probe the possibility of engineering unnatural NRPS modules that contain added Ox domains. It has been shown that entire modules containing Ox domains can be swapped into bimodular model systems, resulting in the release of the anticipated, unnatural oxidized dipeptide products (*28*). In this study, both oxazole- and thiazole-containing molecules were formed when the entire MtaD module was fused to the BacA1 module from the bacitracin biosynthetic pathway. Release of these unnatural compounds was catalyzed successfully by a TE domain fused to the MtaD module. Here, we chose to explore domain exchange, replacing an existing domain within an NRPS module with an Ox domain and evaluating the activity of the resulting chimeric protein.

The location of Ox domains within NRPS modules varies; Ox domains are found inserted within A domains as well as placed at the end of modules, following the T domain. In this study, our focus was on Ox domain placement within the A domain. The Ox domain within MtaD is located between the A_8 and A_9 motifs of the A domain. This is an interesting position because a number of tailoring domains are inserted at this position, including methyltransferases, epimerases, and oxidases (*11*, *17*, *19*, *21*). Because the pyochelin synthetase PchE subunit has an E domain inserted at this position, it appeared probable that the Ox domain from MtaD might be inserted in its place. Not only is the location of the domains the same, but also the two are very close in size (266 amino acids for PchE-E and 271 amino acids for MtaD-Ox) as delineated by secondary structure prediction and alignment with other E and Ox domain sequences. Inspection of a known A domain crystal structure, PheA (*29*), provides insights into why tailoring domain insertion between the A_8 and A_9 motifs might be structurally feasible for the A domain. As shown in Figure 10, this region is unstructured and extends away from the active binding pocket of the enzyme. It is not surprising that alterations are possible in this portion of the enzyme.

Insertion of the MtaD-Ox domain as described in place of the E domain within PchE resulted in chimeric protein construct **1** that proved soluble and loaded with FMN when

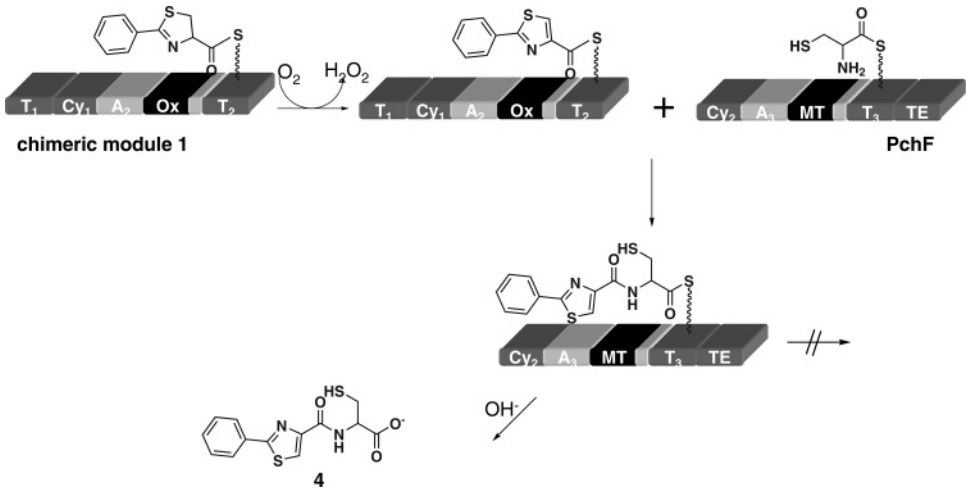

FIGURE 9: Illustration of intermediates covalently tethered to chimeric module **1** and PchF. Thiazoline oxidation and amide bond formation to yield phenylthiazolyl-Cys-*S*-PchF are shown. Hydrolytic product release is not catalyzed by PchF, although base hydrolysis yields free compound 4 (Figure 7). For comparison, the natural pyochelin biosynthetic pathway is shown in Figure 2.

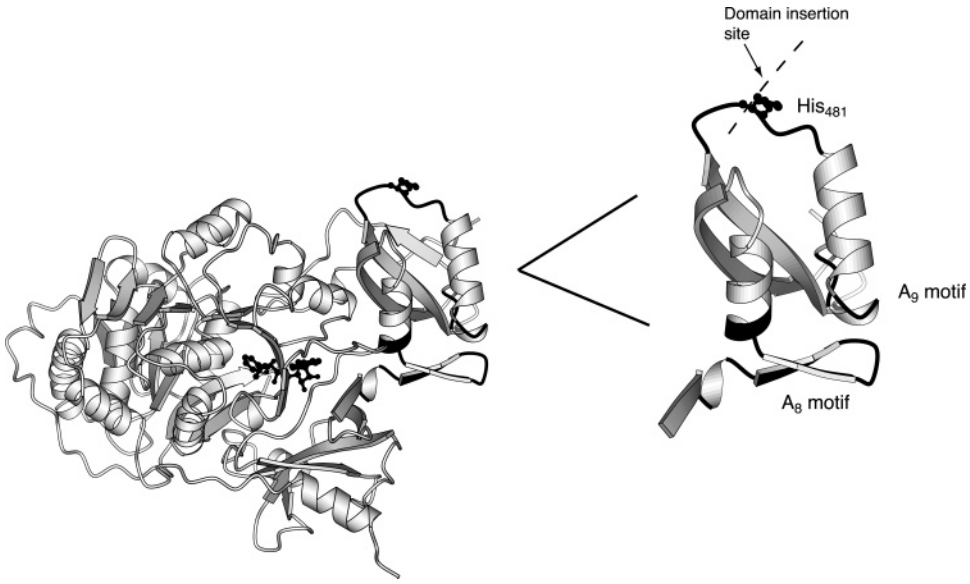

FIGURE 10: Crystal structure of the phenylalanine-activating adenylation domain of gramicidin synthetase 1 (PheA) in complex with phenylalanine and AMP (*29*). The A_8 and A_9 motifs are shown in dark gray just to the right of the binding pocket containing phenylalanine and AMP. The unstructured loop located between the highly conserved A_8 and A_9 motifs is highlighted in black with His_{481} noted. This residue marks the comparable insertion site for MtaD-Ox within PchE, as determined by sequence alignment between PchE and PheA. A comparison with PheA demonstrates that the insertion site is likely unstructured in PchE as well and possibly points away from the active site of the adenylation domain to accommodate an extra domain at this position.

heterologously expressed. Several domains within the construct were impacted by the domain exchange. The Ox domain in this context was only 72% loaded with flavin as compared to 100% for the domain expressed alone, and the Ox turnover was about half as fast when inserted into **1**. Additionally, the A and T domains of PchE showed an even greater decrease in efficiency, suggesting that insertion of the 30-kDa Ox domain had some neighboring effects. Despite these changes in domain activity, **1** proved active and specific, producing only the anticipated oxidized phenylthiazole pyochelin-related intermediate. The insertion of the Ox domain into a foreign A domain did not compromise its ability to act on T-domain-tethered substrates. It is unlikely that the inserted Ox domain is rate-limiting based on analysis of A domain kinetics for **1** as compared to the Ox domain. Additionally, even at early time points, **1** provided only the oxidized intermediate. The Ox domain presented *in cis* yielded only one product, while the Ox domain presented *in trans* gave a mixture of oxidized and nonoxidized products, suggesting that the direct insertion of the Ox domain within the module leads to more efficient oxidation. This conclusion, however, is contingent upon the stereochemistry of the nonoxidized products from the *in trans* reaction; Ox domains typically will only act on thiazolines derived from L-cysteine (*19*). The PchE E domain, known to catalyze the formation of a mixture of thiazoline enantiomers (*21*), might act on a tethered substrate before the Ox domain *in trans*.

It is also not yet clear how insertion of Ox domains impacts chain elongation in NRPS assembly lines. In this case, the oxidized intermediate appeared to be transferred to the downstream PchFTE module, but further processing beyond the amide bond formation to Cys-*S*-PchFTE was not observed, as depicted in Figure 9. It is possible that formation of the second thiazoline ring was catalyzed by PchFTE but

proved sensitive to the alkaline hydrolysis used to release enzyme-bound intermediates. It seems unlikely that a second thiazoline ring was formed and oxidized to the thiazole because such a bithiazole derivative should prove stable even under harsh conditions. Failure to cyclodehydrate phenylthiazolyl-Cys-*S*-PchF would then forestall reduction and N-methylation. These are prerequisites for pyochelin chain maturation and hydrolytic disconnection from PchF. Perhaps the conformation of the planar, oxidized thiazole formed by the chimeric module is not accommodated or recognized by the PchF Cy domain. More investigation of chain elongation will be necessary for engineered assembly lines in which a novel oxidized, heterocyclic natural product variant is desired.

In summary, we have demonstrated that it is possible to form an active, unnatural NRPS module that contains a foreign Ox domain. The insertion of such an Ox domain *in cis* led to specific formation of the predicted oxidized product on that module. It is possible that such an unnatural module might be further optimized using a selection strategy that would complement our design approach. It may also be of future interest to probe Ox domain exchange further, investigating Ox insertion in other pathways. The VibF protein from the vibriobactin biosynthetic pathway catalyzes the formation of dihydroxyphenyl methyloxazoline intermediates (*3*), and this module might prove an interesting place for future exploration of Ox domain portability. While no NRPS Ox domains have been identified to date that naturally catalyze the oxidation of oxazolines, several Ox domains have been shown to oxidize unnatural oxazoline substrate mimics (*19*). Additionally, insertion into the A domain of VibF would test the engineering potential of Ox domains further because there is no existing tailoring domain within VibF. The high tolerance of Ox domains for excision and insertion may render them of real interest in the development of engineered, novel NRPS systems.

ACKNOWLEDGMENT

The authors gratefully acknowledge Rolf Müller and his laboratory (Saarland University, Saarbruecken, Germany) for the gift of a plasmid containing a portion of the *mtaD* gene.

REFERENCES

1. Milne, J. C., Roy, R. S., Eliot, A. C., Kelleher, N. L., Wokhlu, A., Nickels, B., and Walsh, C. T. (1999) Cofactor requirements and reconstitution of microcin B17 synthetase: A multienzyme complex that catalyzes the formation of oxazoles and thiazoles in the antibiotic microcin B17, *Biochemistry 38*, 4768−4781.
2. Quadri, L. E., Keating, T. A., Patel, H. M., and Walsh, C. T. (1999) Assembly of the *Pseudomonas aeruginosa* nonribosomal peptide siderophore pyochelin: *In vitro* reconstitution of aryl-4,2-bisthiazoline synthetase activity from PchD, PchE, and PchF, *Biochemistry 38*, 14941−14954.
3. Keating, T. A., Marshall, C. G., and Walsh, C. T. (2000) Reconstitution and characterization of the *Vibrio cholerae* vibriobactin synthetase from VibB, VibE, VibF, and VibH, *Biochemistry 39*, 15513−15521.
4. Roy, R. S., Gehring, A. M., Milne, J. C., Belshaw, P. J., and Walsh, C. T. (1999) Thiazole and oxazole peptides: Biosynthesis and molecular machinery, *Nat. Prod. Rep. 16*, 249−263.
5. Marahiel, M. A., Stachelhaus, T., and Mootz, H. D. (1997) Modular peptide synthetases involved in nonribosomal peptide synthesis, *Chem. Rev. 97*, 2651−2673.
6. Weber, T., and Marahiel, M. A. (2001) Exploring the domain structure of modular nonribosomal peptide synthetases, *Structure 9*, R3−R9.
7. Stachelhaus, T., Mootz, H. D., Bergendahl, V., and Marahiel, M. A. (1998) Peptide bond formation in nonribosomal peptide biosynthesis, *J. Biol. Chem. 273*, 22773−22781.
8. Keating, T. A., and Walsh, C. T. (1999) Initiation, elongation, and termination strategies in polyketide and polypeptide antibiotic biosynthesis, *Curr. Opin. Chem. Biol. 3*, 598−606.
9. Julien, B., Shah, S., Ziermann, R., Goldman, R., Katz, L., and Khosla, C. (2000) Isolation and characterization of the epothilone biosynthetic gene cluster from *Sorangium cellulosum*, *Gene 249*, 153−160.
10. Molnar, I., Schupp, T., Ono, M., Zirkle, R. E., Milnamow, M., Nowak-Thompson, B., Engel, N., Toupet, C., Stratmann, A., Cyr, D. D., Gorlach, J., Mayo, J. M., Hu, A., Goff, S., Schmid, J., and Ligon, J. M. (2000) The biosynthetic gene cluster for the microtubule-stabilizing agents epothilones A and B from *Sorangium cellulosum* So ce90, *Chem. Biol. 7*, 97−109.
11. Weinig, S., Mahmud, T., and Müller, R. (2003) Markerless mutations in the mxyothiazol biosynthetic gene cluster: A delicate megasynthetase with a superfluous nonribosomal peptide synthetase domain, *Chem. Biol. 10*, 953−960.
12. Du, L., Sanchez, C., Chen, M., Edwards, D. J., and Shen, B. (2000) The biosynthetic gene cluster for the antitumor drug bleomycin from *Streptomyces verticillus* ATCC5003 supporting functional interactions between nonribosomal peptide synthetases and a polyketide synthase, *Chem. Biol. 7*, 623−642.
13. Hamamichi, N., Natrajan, A., and Hecht, S. M. (1992) On the role of individual bleomycin thiazoles in oxygen activation and DNA cleavage, *J. Am. Chem. Soc. 114*, 6278−6291.
14. Henichart, J., Bernier, J., Helbecque, N., and Houssin, R. (1985) Is the bithiazole moiety of bleomycin a classical intercalator? *Nucleic Acids Res. 13*, 6703−6717.
15. Shin-ya, K., Wierbza, K., Matsuo, K., Ohtani, T., Yamada, Y., Furihata, K., Hayakawa, Y., and Seto, H. (2001) Telomestatin, a novel telomerase inhibitor from *Streptomyces anulatus*, *J. Am. Chem. Soc. 123*, 1262−1263.
16. Kim, M., Vankayalapati, H., Shin-ya, K., Wierbza, K., and Hurley, L. H. (2002) Telomestatin, a potent telomerase inhibitor that interacts quite specifically with the human telomeric intramolecular G-quadruplex, *J. Am. Chem. Soc. 124*, 2098−2099.
17. Patel, H. M., and Walsh, C. T. (2001) *In vitro* reconstitution of the *Pseudomonas aeruginosa* nonribosomal peptide synthesis of pyochelin: Characterization of backbone tailoring thiazoline reductase and *N*-methyltransferase activities, *Biochemistry 40*, 9023−9031.
18. Miller, D. A., Luo, L. S., Hillson, N. J., Keating, T. A., and Walsh, C. T. (2002) Yersiniabactin synthetase: A four-protein assembly line producing the nonribosomal peptide/polyketide hybrid siderophore of *Yersinia pestis*, *Chem. Biol. 9*, 333−344.
19. Schneider, T. L., Shen, B., and Walsh, C. T. (2003) Oxidase domains in epothilone and bleomycin biosynthesis: Thiazoline to thiazole oxidation during chain elongation, *Biochemistry 42*, 9722−9730.
20. Stachelhaus, T., Mootz, H. D., and Marahiel, M. A. (1999) The specificity-conferring code of adenylation domains in nonribosomal peptide synthetases, *Chem. Biol. 6*, 493−505.
21. Patel, H. M., Tao, J., and Walsh, C. T. (2003) Epimerization of an L-cysteinyl to a D-cysteinyl residue during thiazoline ring formation in siderophore chain elongation by pyochelin synthetase from *Pseudomonas aeruginosa*, *Biochemistry 42*, 10514−10527.
22. Horton, R. M., Hunt, H. D., Ho, S. N., Pullen, J. K., and Pease, L. R. (1989) Engineering hybrid genes without the use of restriction enzymes: Gene splicing by overlap extension, *Gene 77*, 61−68.
23. Cerletti, P. (1959) Properties of riboflavin phosphates, *Anal. Chim. Acta 20*, 243−250.
24. Reimmann, C., Patel, H. M., Serino, L., Barone, M., Walsh, C. T., and Haas, D. (2001) Essential PchG-dependent reduction in pyochelin biosynthesis of *Pseudomonas aeruginosa*, *J. Bacteriol. 183*, 813−820.
25. Schneider, T. L., Walsh, C. T., and O'Connor, S. E. (2002) Utilization of alternate substrates by the first three modules of the epothilone synthetase assembly line, *J. Am. Chem. Soc. 124*, 11272−11273.
26. Gehring, A. M., Mori, I., Perry, R. D., and Walsh, C. T. (1998) The nonribosomal peptide synthetase HMWP2 forms a thiazoline

ring during biogenesis of yersiniabactin, an iron-chelating virulence factor of *Yersinia pestis*, *Biochemistry 37*, 11637−11650.
27. Nicolaou, K. C., Roschangar, F., and Vourloumis, D. (1998) Chemical biology of epothilones, *Angew. Chem., Int. Ed. 37*, 2015−2045.
28. Duerfahrt, T., Eppelmann, K., Müller, R., and Marahiel, M. A. (2004) Rational design of a bimodular model system for the investigation of heterocyclization in nonribosomal peptide biosynthesis, *Chem. Biol. 11*, 261−271.
29. Conti, E., Stachelhaus, T., Marahiel, M. A., and Brick, P. (1997) Structural basis for the activation of phenylalanine in the nonribosomal biosynthesis of gramicidin S, *EMBO J. 16*, 4174−4183.

BI0481139